AGU ADVANCING EARTH AND SPACE SCIENCE

Geophysical Research Letters®

RESEARCH LETTER
10.1029/2022GL099154

Chromium Cycling in Redox-Stratified Basins Challenges δ^{53}Cr Paleoredox Proxy Applications

David J. Janssen[1,2,3], Jörg Rickli[1,2,4], Martin Wille[1], Oscar Sepúlveda Steiner[3], Hendrik Vogel[1,2], Olaf Dellwig[5], Jasmine S. Berg[6], Damien Bouffard[3,6], Mark A. Lever[7,8], Christel S. Hassler[9,10], and Samuel L. Jaccard[1,2,10]

[1]Institute of Geological Sciences, University of Bern, Bern, Switzerland, [2]Oeschger Centre for Climate Change Research, University of Bern, Bern, Switzerland, [3]Department Surface Waters, Eawag: Swiss Federal Institute of Aquatic Science and Technology, Kastanienbaum, Switzerland, [4]Institute of Geochemistry and Petrology, Department of Earth Sciences, ETH Zurich, Zurich, Switzerland, [5]Marine Geology, Leibniz Institute for Baltic Sea Research, Rostock, Germany, [6]Institute of Earth Surface Dynamics, University of Lausanne, Lausanne, Switzerland, [7]Department of Environmental Systems Science, ETH-Zurich, Zurich, Switzerland, [8]Now at Marine Science Institute, University of Texas at Austin, Port Aransas, TX, USA, [9]Department F.-A. Forel for Environmental and Aquatic Sciences, University of Geneva, Geneva, Switzerland, [10]Institute of Earth Sciences, University of Lausanne, Lausanne, Switzerland

Abstract Chromium stable isotope composition (δ^{53}Cr) is a promising tracer for redox conditions throughout Earth's history; however, the geochemical controls of δ^{53}Cr have not been assessed in modern redox-stratified basins. We present new chromium (Cr) concentration and δ^{53}Cr data in dissolved, sinking particulate, and sediment samples from the redox-stratified Lake Cadagno (Switzerland), a modern Proterozoic ocean analog. These data demonstrate isotope fractionation during incomplete (non-quantitative) reduction and removal of Cr above the chemocline, driving isotopically light Cr accumulation in euxinic deep waters. Sediment authigenic Cr is isotopically distinct from overlying waters but comparable to average continental crust. New and published data from other redox-stratified basins show analogous patterns. This challenges assumptions from δ^{53}Cr paleoredox applications that quantitative Cr reduction and removal limits isotope fractionation. Instead, fractionation from non-quantitative Cr removal leads to sedimentary records offset from overlying waters and not reflecting high δ^{53}Cr from oxidative continental weathering.

Plain Language Summary Chromium stable isotope composition in sediments has been used extensively to understand changes in oxygen availability throughout Earth's history. These reconstructions are built on assumptions of chromium (Cr) transfer between oxic and anoxic waters such that sediments directly reflect oxic surface waters, and therefore trace redox cycling at Earth's surface. However, this has not been tested in modern redox-stratified systems. Here, we show that Cr concentrations and stable isotope compositions deviate from these assumptions. Chromium is neither efficiently removed in anoxic waters, nor do sediments faithfully record water column isotope signatures. A synthesis of new and published observations from euxinic waters indicates these findings appear universal. Previous assumptions of paleo-studies are not supported by modern systems and should be revised.

Key Points:

- Non-quantitative Cr removal at the chemocline drives chromium (Cr) isotope fractionation and the accumulation of light Cr in euxinic deep waters
- Authigenic sediment δ^{53}Cr differs from overlying water, contrary to paleoproxy application assumptions, and is similar to continental crust
- δ^{53}Cr signals in these settings may therefore reflect internal redox processes and not fractionation due to oxidative subaerial weathering

Supporting Information:

Supporting Information may be found in the online version of this article.

Correspondence to:

D. J. Janssen,
david.janssen@eawag.ch

Citation:

Janssen, D. J., Rickli, J., Wille, M., Sepúlveda Steiner, O., Vogel, H., Dellwig, O., et al. (2022). Chromium cycling in redox-stratified basins challenges δ^{53}Cr paleoredox proxy applications. *Geophysical Research Letters*, *49*, e2022GL099154. https://doi.org/10.1029/2022GL099154

Received 13 APR 2022
Accepted 27 SEP 2022

Author Contributions:

Conceptualization: David J. Janssen, Jörg Rickli, Martin Wille, Oscar Sepúlveda Steiner, Hendrik Vogel, Olaf Dellwig, Jasmine S. Berg, Damien Bouffard, Mark A. Lever, Christel S. Hassler, Samuel L. Jaccard
Data curation: David J. Janssen, Jörg Rickli, Oscar Sepúlveda Steiner, Hendrik Vogel, Damien Bouffard
Formal analysis: David J. Janssen, Jörg Rickli, Oscar Sepúlveda Steiner, Olaf Dellwig, Damien Bouffard
Funding acquisition: Samuel L. Jaccard

1. Introduction

Authigenic chromium (Cr) enrichments and Cr stable isotope (δ^{53}Cr) composition in sedimentary deposits are widely used to trace redox conditions throughout Earth's history (Frei et al., 2009; Planavsky et al., 2014; Reinhard et al., 2013; Wei et al., 2020). These applications, which interpret high δ^{53}Cr to signal elevated oxidative weathering of the continents, are based on the redox control of Cr solubility and stable isotope fractionation in aqueous environments. Reduced Cr (Cr(III)) is particle reactive and can be readily removed from the water column (Richard & Bourg, 1991), while oxidized Cr(VI) is soluble, with isotope fractionation resulting in enrichments of isotopically light Cr in Cr(III) (Ellis et al., 2002; Wanner & Sonnenthal, 2013). As a consequence of Cr reduction and removal, natural systems with strong O_2 deficiency are associated with dissolved Cr depletions as well as elevated dissolved δ^{53}Cr (Huang et al., 2021; Moos et al., 2020; Murray et al., 1983; Nasemann et al., 2020; Rue et al., 1997).

Paleo-reconstructions using sedimentary δ^{53}Cr records apply the assumption that Cr is efficiently sequestered into sediment phases under reducing conditions (anoxia or euxinia). Thus, complete (i.e., quantitative) Cr redox

Investigation: David J. Janssen, Jörg Rickli, Martin Wille, Oscar Sepúlveda Steiner, Hendrik Vogel, Olaf Dellwig, Jasmine S. Berg, Damien Bouffard, Mark A. Lever, Christel S. Hassler, Samuel L. Jaccard
Methodology: David J. Janssen
Resources: Martin Wille, Hendrik Vogel, Jasmine S. Berg, Mark A. Lever
Visualization: David J. Janssen, Oscar Sepúlveda Steiner
Writing – original draft: David J. Janssen
Writing – review & editing: David J. Janssen, Jörg Rickli, Martin Wille, Oscar Sepúlveda Steiner, Hendrik Vogel, Olaf Dellwig, Jasmine S. Berg, Damien Bouffard, Mark A. Lever, Christel S. Hassler, Samuel L. Jaccard

conversion prevents isotopic fractionation, resulting in sediment-hosted authigenic δ^{53}Cr equivalent to the overlying water column (Frei et al., 2009, 2020; Reinhard et al., 2013, 2014; Wei et al., 2020). However, the few studies of euxinic waters so far indicate the opposite, that is, enrichment rather than removal of dissolved Cr(III) (Achterberg et al., 1997; Davidson et al., 2020; Emerson et al., 1979), and no data from co-localized euxinic waters and sediments are available. Due to the lack of data on Cr partitioning across redox interfaces and into underlying sediments, isotopic offsets resulting from partial (i.e., non-quantitative) Cr(VI) reduction during removal to sediments have been neglected in δ^{53}Cr paleoproxy interpretations.

Redox-stratified basins are valuable settings to build the geochemical understandings necessary for developing and interpreting paleoproxies for the early stratified oceans. One such system, the meromictic alpine Lake Cadagno (Switzerland) (Figures 1a and 1b), has been used extensively as an analog for the Phanerozoic and Proterozoic oceans (Canfield et al., 2010; Dahl et al., 2010; Ellwood et al., 2019; Xiong et al., 2019) due to the intermediate sulfate levels and sulfidic bottom waters supporting anoxygenic phototrophs in the chemocline (Tonolla et al., 2003). To mechanistically constrain Cr cycling across redox gradients and incorporate these into the Cr-based paleoproxy framework, we present [Cr] and δ^{53}Cr in the water column (total dissolved) and sediments (near-total digests and leachates), along with sinking particulates. These observations question fundamental assumptions inherent to the δ^{53}Cr paleoproxy applications and will help to inform future δ^{53}Cr-based paleo-reconstructions.

2. Study Area and Methods

2.1. Study Area

Lake Cadagno, at 1921 m elevation, is a 21 m deep meromictic alpine lake in Switzerland characterized by a permanent chemocline near 13 m depth. The initially oxic lake formed ∼13,500 YBP. A transition phase persisted between 10,00 and 9,000 YBP, followed by euxinic monimolimnion conditions, which have been generally stable until present (Berg et al., 2022). The lake's distinct geochemistry and microbial communities have been well-characterized. Waters below the chemocline are fed by groundwater input from a karstic system composed of dolomite and gypsum, and are therefore rich in Ca^{2+}, Mg^{2+}, SO_4^{2-} and HCO_3^- relative to overlying waters (Del Don et al., 2001, Figure 1). In anoxic deep waters, dissolved concentrations reach 10^2 μmol kg^{-1} sulfide, ∼3.5 mmol kg^{-1} sulfate, and ∼1 μmol kg^{-1} Fe (e.g., Ellwood et al., 2019, see supplement). High densities of anoxygenic photoautotrophic green and purple sulfur bacteria are found at the chemocline in summer (Tonolla et al., 2003). These bacteria exert control on geochemical gradients in this zone (e.g., S, Fe; Del Don et al., 2001; Berg et al., 2016) and can form a 0.3–1.2 m thick mixed layer through bioconvection during summer (Sepúlveda Steiner et al., 2019, 2021; Sommer et al., 2017).

2.2. Sampling, Sample Purification and Analysis

Dissolved Lake Cadagno water samples were collected on 28–29 August 2017 from a floating platform at the deepest part of the lake. Sediment traps were deployed on 10 July 2017 and recovered on 6 September 2017. Sediments were sampled in summer 2019 and summer 2020 (Berg et al., 2022), freeze dried, and hand milled with an agate mortar and pestle. Baltic Sea samples were collected in the central Landsort Deep (site LD1; 435 m water depth, Häusler et al., 2018) onboard RV Poseidon (POS507, 29 October 2016).

Water column sampling and spiking (with a ^{50}Cr-^{54}Cr double spike) followed standard procedures, and are discussed in Section S.1 in Supporting Information S1. Samples were processed through three stages of column chromatography: (i) Fe removal using AG1-X8 resin in 6.4 M HCl (Scheiderich et al., 2015), followed by (ii) anion and (iii) cation chromatography as described elsewhere (Janssen et al., 2020; Nasemann et al., 2020; Rickli et al., 2019). Sediment near-total digests were prepared using inverse aqua regia with H_2O_2. Authigenic sediment phases (primarily organic matter, potentially also sulfides, Figure 2a) were targeted with a 30% v/v H_2O_2 leach at pH = 2 following Rauret et al. (1999) (see Section S.1 in Supporting Information S1). Leach and digest subsamples were spiked with a ^{50}Cr-^{54}Cr double spike, dried and processed through steps (i) and (iii). Reagents were either sub-boiling distilled (acids) or Romil UpA and Fisher Optima grade (H_2O_2). Ancillary data are described in the supplement.

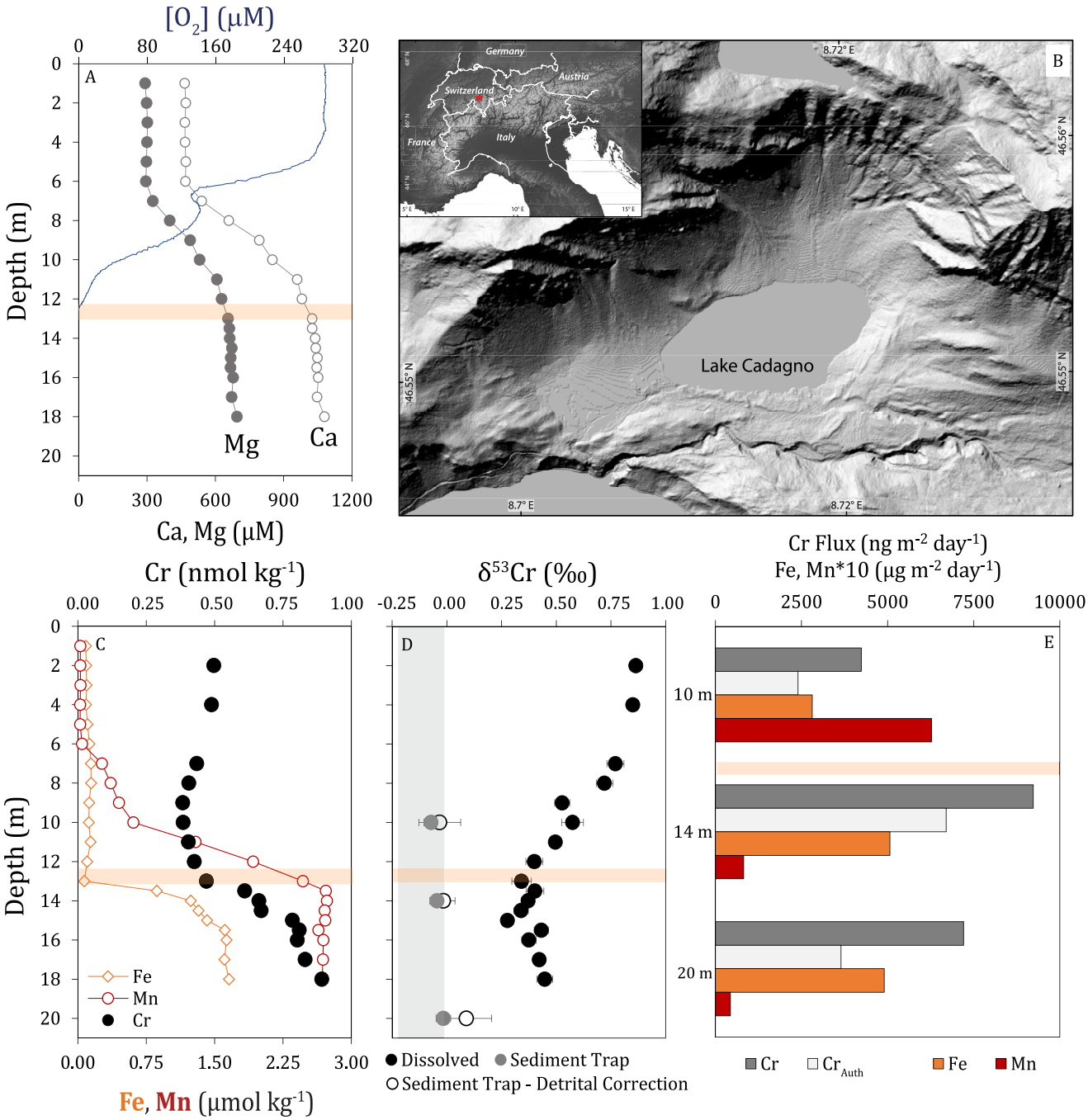

Figure 1. Water column data. (a): $[O_2]$, [Ca] and [Mg]. (b): map showing the location of Lake Cadagno. (c): dissolved [Cr], [Fe] and [Mn]. (d): dissolved and sediment trap $\delta^{53}Cr$ (uncorrected and corrected for detrital chromium (Cr), see Section S.5 in Supporting Information S1). (e): Sediment trap Cr, Fe and Mn fluxes (note different depth range). The orange box in (a and c–e) indicates the chemocline. The gray box in (d) indicates average detrital $\delta^{53}Cr$ (Schoenberg et al., 2008).

Sediment trap fluxes are calculated with and without corrections for lithogenic contributions (Figures 1 and 2, Table 1). Uncertainties on corrected data (pCr_{Auth}) follow standard error propagation using lithogenic Cr/Al (Rudnick & Gao, 2014) and $\delta^{53}Cr = -0.12 \pm 0.1$ ‰ (Schoenberg et al., 2008). Such corrections, which rely on normalizations to major crustal elements considered minimally mobile (e.g., Al), are complicated by the authigenic components of these elements in Lake Cadagno (Figures S6 and S7 in Supporting Information S1). Therefore, these corrections underestimate pCr_{Auth} and overestimate $\delta^{53}Cr_{Auth}$, with true authigenic values lying between the corrected and uncorrected data (See Section S.5 in Supporting Information S1). Detrital corrections

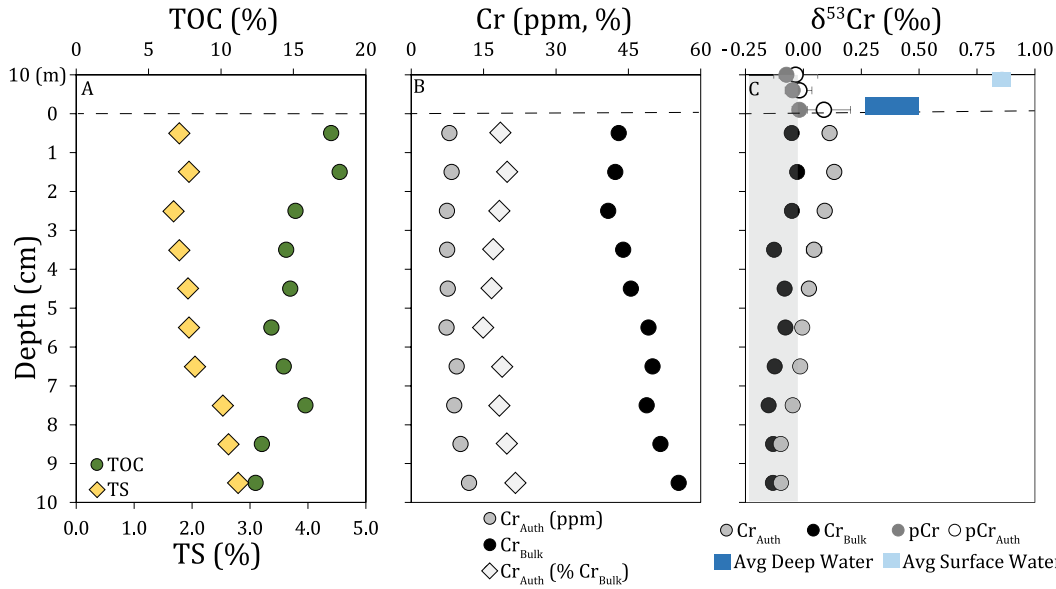

Figure 2. Near-surface sediment data. (a): bulk sediment parameters (TOC, TS). (b): near-total digest (Cr_{Bulk}) and leach (Cr_{Auth}) concentrations, and Cr_{Auth} as % Cr_{Bulk}. (c): $\delta^{53}Cr_{Bulk}$ and $\delta^{53}Cr_{Auth}$ with average surface and deep water dissolved $\delta^{53}Cr$ and sediment trap $\delta^{53}Cr$ (total and detrital-corrected), along with average detrital $\delta^{53}Cr$ (gray box).

were not applied to sediment leach data as chemical leaches were more gentle than sediment trap digests (See Section S.1.2 in Supporting Information S1) enhancing the impact of authigenic phases of the normalizing element and exacerbating artifacts from improper corrections (Figures S6 and S7 in Supporting Information S1).

Purified $\delta^{53}Cr$ samples were dissolved in 0.7–1 mL 0.5 M HNO_3 and analyzed with a Neptune Plus MC-ICP-MS (ThermoFisher) (Rickli et al., 2019). Internal sample uncertainty (2 SEM) and session reproducibility from NIST standards ($n \approx 10$, 2 SD) is typically around 0.02–0.03 ‰. External uncertainty has previously been estimated at ±0.033 ‰ for full sample replicates (Janssen et al., 2020). Pure standard reference materials (Merck Cr(III)

Table 1
Sediment Trap, Diffusive and Burial Fluxes

	Depth	pCr				pCr_{Auth}			
Downward fluxes	m	ng Cr	ng Cr m^{-2} day^{-1}	$\delta^{53}Cr$	2SEM	ng Cr	ng Cr m^{-2} day^{-1}	$\delta^{53}Cr$	2SEM
Sediment Trap	10	3.2×10^3	4.2×10^3	−0.07	0.03	1.8×10^3	2.4×10^3	−0.03	0.09
Sediment Trap	14	7.0×10^3	9.2×10^3	−0.05	0.03	5.1×10^3	$\mathbf{6.7 \times 10^3}$	−0.02	0.05
Sediment Trap	20	5.4×10^3	7.2×10^3	−0.02	0.03	2.8×10^3	3.6×10^3	0.09	0.11
	Euxinic zone [Cr]	Chemocline base [Cr]	Δ[Cr]	ΔZ	K	Flux	Flux		
Upward Fluxes	nmol kg^{-1}	nmol kg^{-1}	nmol cm^{-3}	cm	cm^2 s^{-1}	nmol cm^{-2} s^{-1}	ng m^{-2} d^{-1}		
Turbulent Diffusion	0.67	0.47	0.0002	150	1.1×10^{-1}	1.4×10^{-7}	$\mathbf{6.4 \times 10^3}$		
Molecular Diffusion	0.67	0.47	0.0002	150	3.4×10^{-6}	4.6×10^{-12}	2.7×10^{-1}		
	Sediment Acc. Rate[1]	Wet Sed. Density (ρ)	Porosity (β)	Cr_{Auth}	F_{Burial}	F_{Burial}	F_{Burial}		
Cr burial	mm yr^{-1}	g cm^{-3}	g H_2O g wet $sed.^{-1}$	ppm	nmol cm^{-2} y^{-1}	ng cm^{-2} y^{-1}	ng m^{-2} d^{-1}		
Authigenic Cr Burial	4–6	2.30	0.33	8	0.9–1.4	49–74	$1.3–2.0 \times 10^3$		

Note. Fluxes to and from the chemocline are in bold. Sediment trap data include both total (pCr) and detrital-corrected (pCr_{Auth}) fluxes (See Section S.5 in Supporting Information S1). Upward turbulent diffusive fluxes of dissolved [Cr] are based on [Cr] gradients from the chemocline to 1.5 m below the chemocline. [1]Birch et al., 1996. See Section S.3.3 in Supporting Information S1 for further details on authigenic burial estimates.

standard, this study: $\delta^{53}Cr = -0.45 \pm 0.03$ ‰, $n = 10$; $\delta^{53}Cr = -0.44 \pm 0.02$ ‰, Schoenberg et al., 2008) and USGS reference materials (Table S3 in Supporting Information S1) agree with published values.

3. Lake Cadagno Results and Discussion

3.1. Water Column

Dissolved [Cr] is stable in the surface mixed layer ([Cr] = 0.5 nmol kg^{-1}, Figure 1c). A broad [Cr] minimum is found at 8–11 m depth, above the chemocline (~12–13 m in summer 2017, Figure S1 in Supporting Information S1; Sepúlveda Steiner et al., 2021). Particulate Fe and Mn oxides form within and above the chemocline in Lake Cadagno, driven by upward transport of dissolved Fe(II)—a known Cr reductant (Richard & Bourg, 1991; Wanner & Sonnenthal, 2013)—and Mn(II) from the anoxic zone (Ellwood et al., 2019). As these oxides sink below the chemocline, they are reductively dissolved within the anoxic zone, and particulate Fe sulfides are formed (Ellwood et al., 2019). The [Cr] minimum lies within the most stratified portion of the water column (Figure S2 in Supporting Information S1) and corresponds to depths with enhanced formation and sinking of Fe and Mn oxides (see figure 5 in Ellwood et al., 2019). Therefore the [Cr] minimum is mechanistically consistent with Cr reduction coupled to Fe oxidation followed by Cr scavenging onto metal oxides.

Chromium concentrations begin increasing just above the chemocline, exceeding surface concentrations immediately below the chemocline. Dissolved [Fe] and [Mn] also increase over this range, with the [Cr] increase more closely mirroring [Fe] (Figure 1c). Matching [Cr], $\delta^{53}Cr$ is stable in the surface mixed layer ($\delta^{53}Cr = +0.86$ ‰) (Figure 1d), with the isotopically heavy dissolved Cr signal likely reflecting surface water input to the lake, consistent with expectations from oxidative terrestrial weathering and global observations of riverine $\delta^{53}Cr$ (Wei et al., 2020). $\delta^{53}Cr$ decreases with depth, indicating the accumulation of isotopically light Cr in deep waters following Cr release during metal oxide reduction.

Sinking fluxes of authigenic particulate Cr (pCr_{Auth}) increase near the chemocline, with maximum fluxes observed in the 14 m trap. Exported pCr is isotopically lighter than dissolved Cr, with $\Delta^{53}Cr_{patriculate\text{-}dissolved} \approx -0.6 \pm 0.1$ ‰ near the chemocline. This is comparable to net fractionations observed in other natural systems, but is much lower than theoretical values observed in lab studies (e.g., Wanner & Sonnenthal, 2013), which likely reflects incomplete removal of reduced Cr resulting in lower apparent fractionation factors for Cr reduction and removal (Huang et al., 2021; Nasemann et al., 2020; Wang, 2021). Isotopically, pCr_{Auth} is indistinguishable from the lithogenic background ($\delta^{53}Cr = -0.12 \pm 0.10$ ‰, Schoenberg et al., 2008). Export fluxes of pCr_{Auth} and pMn decrease with depth in the euxinic zone (Figures 1e and Table 1; Table S2 in Supporting Information S1), while pFe species shift from oxide-dominated above the chemocline to sulfides below (Berg et al., 2022; Ellwood et al., 2019), suggesting an Fe-Mn-oxyhydroxide shuttle and resulting in much of the Cr exported across the chemocline being released before the deepest sediment trap (20 m). The behavior of pCr is thus consistent with dissolved data indicating Cr release and accumulation in the euxinic zone following reduction of Fe and Mn oxides. Despite depth-dependent variability in pCr_{Auth}, exported $\delta^{53}Cr$ is uniform within analytical uncertainty, indicating no fractionation during Cr release.

Deep layers of euxinic water bodies are assumed to remain quiescent given the strong stratification, and therefore the vertical gradient of [Cr] should be smoothed by an upward molecular diffusive flux. However, the pCr_{Auth} export (~6.7×10^3 ng Cr m^{-2} day^{-1}) is orders of magnitude larger than the molecular flux of dissolved Cr (Table 1, Section S.3 in Supporting Information S1) while the observed [Cr] depletion is subtle. Despite the apparent quiescence of the deep interiors of lakes, various physical processes maintain a moderate and intermittent energetic structure (Saggio & Imberger, 2001), including in Lake Cadagno (Wüest, 1994). Here our concurrent microstructure observations indicate that vertical fluxes are sustained by turbulent diffusivity (K_{oc}, Osborn & Cox, 1972), with a mean K_{oc} in the layer of interest of 10^{-1} cm^2 s^{-1} (Figure S2 in Supporting Information S1; four orders of magnitude larger than molecular diffusivity). This results in upward turbulent flux estimates comparable to sinking pCr fluxes, while the authigenic burial flux is comparatively smaller (~25% of turbulent and particulate fluxes, Table 1). The background turbulence thereby explains Cr profiles and, particularly, the lack of a pronounced [Cr] minimum and local $\delta^{53}Cr$ maximum above the chemocline, due to the substantial upward turbulent transport of isotopically light Cr. The result is similar to "cryptic" cycles, where rapid and localized

redox cycling masks the expected biogeochemical signals (e.g., Berg et al., 2016), though rather as a larger-scale physical-geochemical transport cycle.

Observed deep water [Cr] enrichments likely reflect the integrated accumulation of Cr released from sinking particles and near-surface sediments as well as the potential contribution from groundwater (Del Don et al., 2001), with concentrations further modified by turbulent mixing. As there is no modification of particulate $\delta^{53}Cr$ with depth, released Cr must be of similar isotope composition as the particulates ($\delta^{53}Cr \approx 0$ ‰). Therefore, any groundwater Cr must be isotopically heavier than 0 ‰ (see Section S.4 in Supporting Information S1). However, while subaquatic springs likely influence specific aspects of Lake Cadagno deep water [Cr] and $\delta^{53}Cr$, other euxinic basins exhibit similar large-scale [Cr] and $\delta^{53}Cr$ depth-trends (see below). Therefore, a shared set of geochemical and physical controls likely shape the common large-scale [Cr] and $\delta^{53}Cr$ trends across diverse euxinic basins.

3.2. Sediments

Authigenic Cr (Cr_{Auth}) in near-surface sediments is isotopically lighter than deep water, with similar $\delta^{53}Cr$ as sinking particles (Figure 2). We do not observe strong [Cr_{Auth}] enrichments relative to [Cr_{Bulk}], despite stably euxinic deep waters and large Cr fluxes from the chemocline, and Cr_{Auth} burial fluxes are small relative to chemocline particulate fluxes, reflecting significant Cr release from sinking particles (Table 1, Section S.3.3 in Supporting Information S1). Sediment Mn and Fe(III) content is low relative to sinking particles (Figure 1, Ellwood et al., 2019; Berg et al., 2022), supporting a Fe-Mn-oxyhydroxide shuttle for Cr, with Cr release following oxide dissolution. Bulk sediment $\delta^{53}Cr$ ($\delta^{53}Cr_{Bulk}$) is indistinguishable from average continental crust (-0.12 ± 0.10 ‰, Schoenberg et al., 2008) at all depths. $\delta^{53}Cr_{Auth}$ is slightly higher than crustal signatures in the uppermost sediments; however, $\delta^{53}Cr_{Auth}$ decreases with sediment depth and is indistinguishable from this inventory below 5 cm. $\delta^{53}Cr_{Bulk}$ and $\delta^{53}Cr_{Auth}$ converge in the upper 10 cm of the sediment, suggesting modification of $\delta^{53}Cr$ through early diagenesis (sedimentation rates ~4–6 mm yr^{-1}, Birch et al., 1996), similar to reports of Cr homogenization in black shales (Frank, et al., 2020).

While surface sediment $\delta^{53}Cr_{Auth}$ equals sinking particulate $\delta^{53}Cr$, non-quantitative water column Cr removal results in isotope fractionation and an offset between sediments and dissolved $\delta^{53}Cr$. This fractionation, along with potential early diagenetic modification, leads coincidentally to a $\delta^{53}Cr_{Auth}$ equivalent to detrital reservoirs (Figure 2). $\delta^{53}Cr_{Auth}$ is approximately 0.6 ‰ lower than dissolved $\delta^{53}Cr$ in Lake Cadagno at the [Cr] minimum; however, variable dissolved $\delta^{53}Cr$ results in inconsistent offsets between $\delta^{53}Cr_{Auth}$ and surface, deep and chemocline dissolved $\delta^{53}Cr$. [Cr_{Bulk}] and $\delta^{53}Cr_{Bulk}$ in sapropel samples, obtained from a sediment core spanning the last ~12 ka (Berg et al., 2022) remain relatively stable with depth. $\delta^{53}Cr_{Bulk}$ is indistinguishable from lithogenic background and $\delta^{53}Cr_{Auth}$ is indistinguishable from or only slightly heavier than lithogenic background (Figure S5 in Supporting Information S1). Thus, despite deposition in an anoxic basin below an oxidizing atmosphere, sediment $\delta^{53}Cr_{Bulk}$ and $\delta^{53}Cr_{Auth}$ provide no isotopically heavy Cr record (reflecting oxidative weathering and high dissolved $\delta^{53}Cr$). These data imply that in other redox-stratified settings, an isotopically heavy dissolved $\delta^{53}Cr$ pool does not necessarily result in isotopically heavy $\delta^{53}Cr_{Auth}$ or $\delta^{53}Cr_{Bulk}$ records, and that constraints on water column fractionation are needed to reconstruct dissolved $\delta^{53}Cr$ of overlying waters and oxidative weathering processes from sedimentary $\delta^{53}Cr$ records.

4. Synthesis of Redox-Stratified Systems

$\delta^{53}Cr$ has received significant attention as a paleoproxy for O_2 availability, especially in the Proterozoic. While Lake Cadagno is a promising analogue for biogeochemical cycling in the Proterozoic ocean, it remains a small Alpine lake with unique physical and biogeochemical cycling. To assess the relevance of these data to other modern redox-stratified systems and to oceanic systems throughout geologic time, we compiled new dissolved [Cr] and $\delta^{53}Cr$ data from the weakly euxinic Landsort Deep site in the Baltic Sea (Häusler et al., 2018), together with published [Cr] data from other redox-stratified basins (Figure 3).

In the Landsort Deep, Cr is removed near the chemocline (Figure 3b, Table S7 in Supporting Information S1), coincident with a maximum in particulate Fe and Mn oxides. High dissolved [Cr] and low $\delta^{53}Cr$ are found in underlying waters where dissolved [Fe] and [Mn] reach μM levels, indicating an accumulation of isotopically light Cr in euxinic waters as in Lake Cadagno. These data support isotope fractionation during non-quantitative

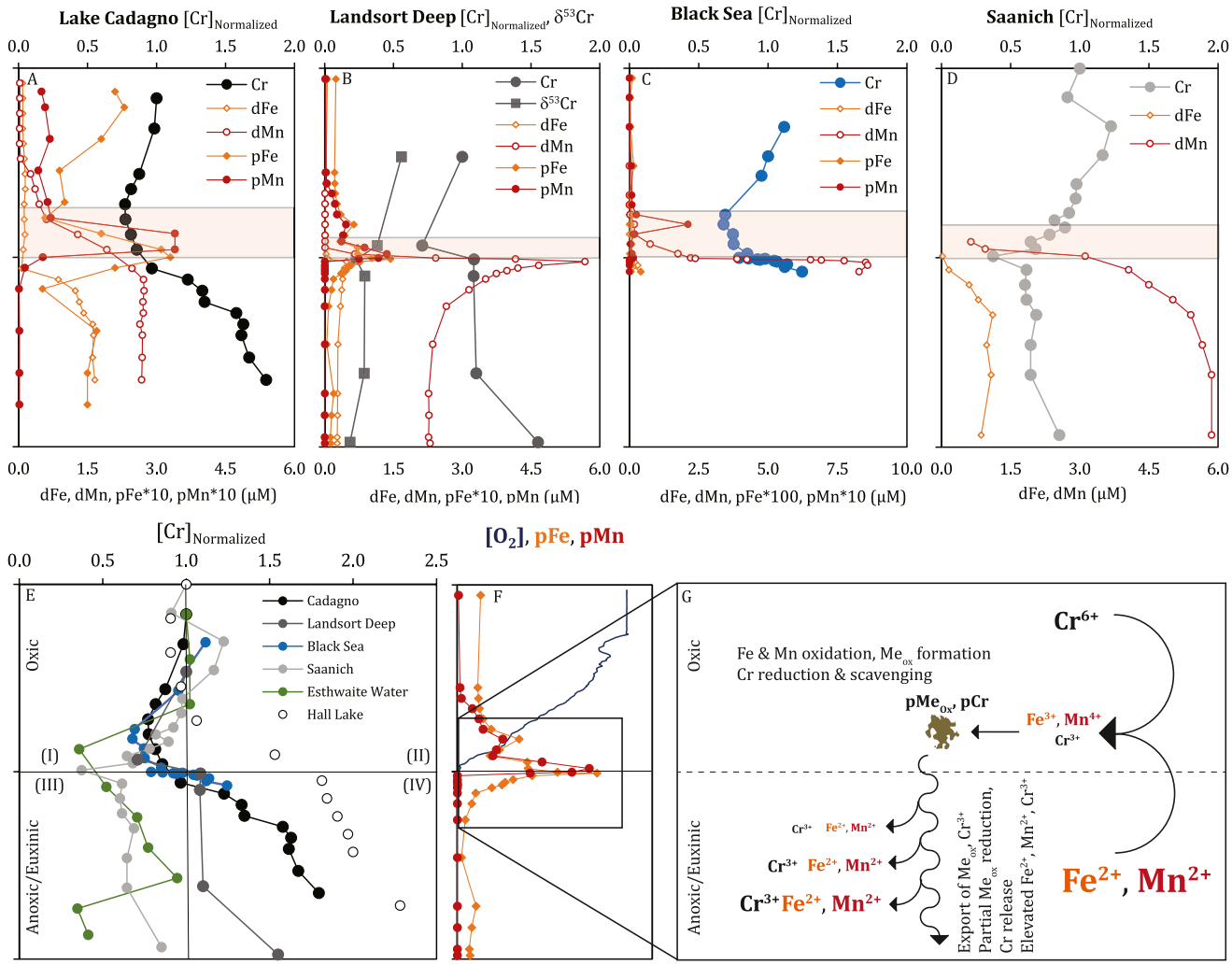

Figure 3. Compilation of anoxic basin data with conceptual mechanistic diagram. Chromium, Fe (orange) and Mn (red) concentrations in the dissolved (open circles, dFe and dMn) and particulate (filled circles, pFe and pMn) phases from Lake Cadagno ((a), black, this study, pFe and pMn: Ellwood et al., 2019), Landsort Deep ((b), dark gray, this study), the Black Sea ((c), blue, Cr: Mugo, 1997, Fe and Mn: Lewis & Landing, 1991), and Saanich Inlet ((d), Emerson et al., 1979, light gray, only dissolved data). (e) combines (a–d) with Esthwaite Water (green, Achterberg et al., 1997) and Hall Lake (white, Balistrieri et al., 1994). In (a)–(f), the *y*-axis ranges from the surface to sediments, with the chemocline at the center. In (a–e), [Cr] is normalized to surface concentrations. The orange shading in (a–d) indicates the zone of enhanced Fe and Mn redox cycling above the chemocline. (f–g) show a schematic of metal cycling in this zone, using Landsort Deep data (f) (see Table S8 in Supporting Information S1).

Cr reduction and removal via scavenging onto metal oxides slightly above the chemocline, with Cr release following oxide reduction in euxinic waters and/or surface sediments.

Data from other redox-stratified basins are similar, despite wide ranges in dissolved H_2S (10^{0}–10^{2} μmol kg^{-1}) and Fe (10^{-2}–10^{2} μmol kg^{-1}) concentrations and Fe/H_2S (10^{-4}–10^{3}) (Table S9 in Supporting Information S1). This includes Lake Cadagno and the Landsort Deep, Saanich Inlet (Emerson et al., 1979, BC Canada, see also Davidson et al., 2020), the Black Sea (Mugo, 1997), Esthwaite Water (UK, Achterberg et al., 1997) and Hall Lake (Wa USA; Balistrieri et al., 1994) (Figures 3a–3e). These can be more directly compared by normalizing profiles to $[Cr]_{surface}$ and relative depth above and below the chemocline, creating four quadrants: (I) $[Cr] < [Cr]_{surface}$ in oxic waters, (II) $[Cr] > [Cr]_{surface}$ in oxic waters, (III) $[Cr] < [Cr]_{surface}$ in anoxic waters, and (IV) $[Cr] > [Cr]_{surface}$ in anoxic waters (Figure 3e). All environments lie within (I) slightly above the chemocline, indicating non-quantitative Cr removal. Anoxic deep waters fall into quadrant (IV) in most settings, indicating Cr accumulation rather than removal. Basins with only seasonal anoxia (Saanich Inlet, Esthwaite Water) differ, showing a

slight increase in $[Cr]_{Normalized}$ just above the chemocline but remaining in zone (III) at depth. This may indicate insufficient time to allow Cr accumulation through the Fe-Mn shuttle, due to their only seasonally anoxic nature.

This compilation from diverse permanently and seasonally anoxic systems confirms the general trends observed in Lake Cadagno—(i) non-quantitative Cr removal above the chemocline (~20–60% of $[Cr]_{surface}$), suggesting isotope fractionation and the transport of low $\delta^{53}Cr$ to anoxic waters, and (ii) Cr accumulation in anoxic deep waters indicating poor sequestration of Cr into sediments. Therefore, reconstructions of water column or weathering $\delta^{53}Cr$ signals from sediments deposited in these environments require accounting for fractionation during Cr removal as well as internal cycling resulting in variable water column $\delta^{53}Cr$.

Chromium depletions consistently occur above the chemocline, coincident with elevated dissolved and particulate [Fe] and [Mn] (orange box in Figures 3a–3d). The sharpness of the Cr depletion above and subsequent increase below the chemocline can be explained by natural variability in the systems (see also Dellwig et al., 2012), including absolute depth ranges (10–10^3 m), the relative width of the Fe-Mn redox zone (orange box height, Figures 3a–3d) and upward diffusive transport. Shallower systems (e.g., Hall and Cadagno Lakes), thicker Fe-Mn redox zones, and elevated diffusivity correspond with broader Cr minima and more gradual Cr increases below the chemocline.

In agreement with previous studies (e.g., Balistrieri et al., 1994; Mugo, 1997), the consistent Cr minimum in the zone of intense Fe-Mn redox cycling supports the widespread control of these metals on Cr removal in anoxic systems, whereby Cr reduction coupled to Fe oxidation and subsequent Cr(III) scavenging on particulate metal oxides drives Cr removal (Figures 3f and 3g), followed by oxide reduction and Cr release in the anoxic zone or near the sediment surface. The broadly similar Cr trends across these diverse freshwater and marine systems indicates that our data from Cadagno are generally relevant to other systems and can be used to revise the interpretational framework of $\delta^{53}Cr$ paleoproxy applications. Specifically, these data indicate that:

1. Cr is partially removed above the chemocline, but is not efficiently removed from the water column in anoxic systems, both at and below the chemocline
2. Dissolved Cr generally accumulates in anoxic deep water
3. Sediments from redox-stratified basins may not always show high $[Cr_{Auth}]$ enrichments
4. Reconstructing water column $\delta^{53}Cr$ from $\delta^{53}Cr_{Auth}$ within these settings requires accounting for variable water column $\delta^{53}Cr$, fractionation during Cr removal and early diagenesis
5. $\delta^{53}Cr_{Auth}$ within these settings may therefore not directly reflect Cr fractionation originating from oxidative subaerial weathering

5. Conclusions and Implications

Available data across a range of redox-stratified marine and lacustrine settings share fundamental features—namely, local [Cr] minima with non-quantitative Cr removal slightly above the chemocline, and increasing [Cr] below—with permanently anoxic basins showing deep water dissolved Cr accumulation rather than efficient removal. Given the isotope fractionation associated with Cr reduction, non-quantitative removal suggests that sedimentary authigenic $\delta^{53}Cr$ should not match the water column, contrasting previous assumptions (e.g., Frei et al., 2009, 2020; Reinhard et al., 2013, 2014; Wei et al., 2020). Instead, sediment $\delta^{53}Cr_{Auth}$ is isotopically offset from the water column, a factor that must be considered for paleoreconstructions. Furthermore, variable water column $\delta^{53}Cr$, as well as potential early diagenetic modification of $\delta^{53}Cr_{Auth}$, suggests there is no consistent offset between $\delta^{53}Cr_{Auth}$ and water column $\delta^{53}Cr$. Indeed, our Lake Cadagno data show that sinking particulate $\delta^{53}Cr$ is isotopically comparable to sediment $\delta^{53}Cr_{Auth}$, while dissolved $\delta^{53}Cr$ decreases from surface waters to euxinic deep waters, and therefore dissolved $\delta^{53}Cr$ differs from $\delta^{53}Cr_{Auth}$ by variable extents.

Despite a strongly oxidizing atmosphere throughout the entire history of Lake Cadagno, we find no significantly fractionated sediment $\delta^{53}Cr_{Auth}$. Evidently, oxidative weathering does not necessarily result in high $\delta^{53}Cr_{Auth}$. To the contrary, the relatively small ranges of dissolved $\delta^{53}Cr$ throughout modern systems (surface waters ≈ +0.2 to +1.2 ‰, Wei et al., 2020; Horner et al., 2021) coupled with effective fractionation for the reduction and removal of Cr ($\Delta^{53}Cr \approx -0.4$ to -1.3 ‰; this study; Janssen et al., 2020, 2021; Moos et al., 2020; Nasemann et al., 2020; Huang et al., 2021; Wang, 2021) indicate that authigenic sedimentary $\delta^{53}Cr$ records could easily be comparable to unfractionated continental crust ($\delta^{53}Cr = -0.12 \pm 0.10$ ‰, Schoenberg et al., 2008). In other words, Cr removal from a water column inventory of +0.2 to +1.2 ‰, with a $\Delta^{53}Cr_{particle\text{-}dissolved}$ of −0.4 to −1.3 ‰ is expected

to yield an authigenic sedimentary $\delta^{53}Cr$ that is, at times, within the range of −0.2 to 0.0 ‰. Consequently, caution should be used in the interpretation of $\delta^{53}Cr$ records from redox-stratified basins, which reflect local redox-related fractionation processes superimposed on oxidative subaerial weathering signals.

Data Availability Statement

Data are presented in the Supporting Information S1 and Table 1. Vertical microstructure data for turbulent diffusion estimations is available at https://doi.org/10.5281/zenodo.3507638. Chemical and CTD data are also available in the following open access datasets in the Zenodo repository: http://doi.org/10.5281/zenodo.7125831 and http://doi.org/10.5281/zenodo.7127882, respectively.

Acknowledgments
The authors thank Nathalie Dubois for providing sediment traps and Alois Zwyssig for assistance deploying and recovering the traps. We thank the Piora Centro Biologia Alpina (CBA) for use of the sampling platform and housing as well as Samuele Roman for logistical support. We thank Julia Gajic for TC/TIC/TN/TS analyses, Patrick Kathriner for dissolved Ca and Mg analyses, and the crew and captain of *RV Poseidon* for assistance with Baltic Sea sampling. Elena Serra provided the map used in Figure 1. This manuscript was improved by comments from three anonymous reviewers. Funding was provided by the Swiss National Science Foundation (Grant PP00P2_172915) and the European Research Council (ERC CoG—SCrIPT Grant 819139) to SLJ. Chromium data were obtained on a Neptune MC-ICP-MS at the University of Bern acquired with funds from the NCCR PlanetS supported by SNSF Grant 51NF40-141881. O.S.S. and D.B. were supported by SNSF Grant 179264 (BioCad). The specific contributions of each author are as follows: DJJ, JR and SLJ designed the study, with input from MW, HV and CSH. DJJ processed and analyzed all Cr samples. JR measured ancillary metal data for water column (dissolved and sediment trap) and sediment leach samples. JR, CSH and SLJ conducted Lake Cadagno water column sampling. JB, ML and HV coordinated sampling for the 8 m sediment core and MW and HV sampled the short core for near surface sediments. OD conducted Landsort Deep water column sampling and produced ancillary Landsort Deep data. MW conducted near-total sediment digests and DJJ conducted sediment leaches. OSS and DB conducted physical limnological investigations of Lake Cadagno, coordinated multiparameter profile measurements presented in Figure S1 in Supporting Information S1, and derived turbulent diffusivity values. DJJ led interpretations of the data and preparation of the manuscript, with input from all co-authors.

References

Achterberg, E. P., Van Den Berg, C. M., Boussemart, M., & Davison, W. (1997). Speciation and cycling of trace metals in Esthwaite water: A productive English lake with seasonal deep-water anoxia. *Geochimica et Cosmochimica Acta*, *61*(24), 5233–5253. https://doi.org/10.1016/S0016-7037(97)00316-5

Balistrieri, L. S., Murray, J. W., & Paul, B. (1994). The geochemical cycling of trace elements in a biogenic meromictic lake. *Geochimica et Cosmochimica Acta*, *58*(19), 3993–4008. https://doi.org/10.1016/0016-7037(94)90262-3

Berg, J. S., Lepine, M., Laymand, E., Han, X., Vogel, H., Morlock, M. A., et al. (2022). Ancient and modern geochemical signatures in the 13, 500-year sedimentary record of lake Cadagno. *Frontiers of Earth Science*, *9*, 754888. https://doi.org/10.3389/feart.2021.754888

Berg, J. S., Michellod, D., Pjevac, P., Martinez-Perez, C., Buckner, C. R., Hach, P. F., et al. (2016). Intensive cryptic microbial iron cycling in the low iron water column of the meromictic Lake Cadagno. *Environmental Microbiology*, *18*(12), 5288–5302. https://doi.org/10.1111/1462-2920.13587

Birch, L., Hanselmann, K. W., & Bachofen, R. (1996). Heavy metal conservation in Lake Cadagno sediments: Historical records of anthropogenic emissions in a meromictic alpine lake. *Water Research*, *30*(3), 679–687. https://doi.org/10.1016/0043-1354(95)00231-6

Canfield, D. E., Farquhar, J., & Zerkle, A. L. (2010). High isotope fractionations during sulfate reduction in a low-sulfate euxinic ocean analog. *Geology*, *38*(5), 415–418. https://doi.org/10.1130/G30723.1

Dahl, T. W., Anbar, A. D., Gordon, G. W., Rosing, M. T., Frei, R., & Canfield, D. E. (2010). The behavior of molybdenum and its isotopes across the chemocline and in the sediments of sulfidic Lake Cadagno, Switzerland. *Geochimica et Cosmochimica Acta*, *74*(1), 144–163. https://doi.org/10.1016/j.gca.2009.09.018

Davidson, A. B., Semeniuk, D. M., Koh, J., Holmden, C., Jaccard, S. L., Francois, R., & Crowe, S. A. (2020). A $Mg(OH)_2$ coprecipitation method for determining chromium speciation and isotopic composition in seawater. *Limnology and Oceanography: Methods*, *18*(1), 8–19. https://doi.org/10.1002/lom3.10342

Del Don, C., Hanselmann, K. W., Peduzzi, R., & Bachofen, R. (2001). The meromictic Alpine lake Cadagno: Orographical and biogeochemical description. *Aquatic Sciences*, *63*(1), 70–90. https://doi.org/10.1007/PL00001345

Dellwig, O., Schnetger, B., Brumsack, H. J., Grossart, H. P., & Umlauf, L. (2012). Dissolved reactive manganese at pelagic redoxclines (part II): Hydrodynamic conditions for accumulation. *Journal of Marine Systems*, *90*(1), 31–41. https://doi.org/10.1016/j.jmarsys.2011.08.007

Ellis, A. S., Johnson, T. M., & Bullen, T. D. (2002). Chromium isotopes and the fate of hexavalent chromium in the environment. *Science*, *295*(5562), 2060–2062. https://doi.org/10.1126/science.1068368

Ellwood, M. J., Hassler, C., Moisset, S., Pascal, L., Danza, F., Peduzzi, S., et al. (2019). Iron isotope transformations in the meromictic Lake Cadagno. *Geochimica et Cosmochimica Acta*, *255*, 205–221. https://doi.org/10.1016/j.gca.2019.04.007

Emerson, S., Cranston, R. E., & Liss, P. S. (1979). Redox species in a reducing fjord: Equilibrium and kinetic considerations. *Deep-Sea Research A.*, *26*(8), 859–878. https://doi.org/10.1016/0198-0149(79)90101-8

Frank, A. B., Klaebe, R. M., Löhr, S., Xu, L., & Frei, R. (2020). Chromium isotope composition of organic-rich marine sediments and their mineral phases and implications for using black shales as a paleoredox archive. *Geochimica et Cosmochimica Acta*. *270*, 338–359. https://doi.org/10.1016/j.gca.2019.11.035

Frei, R., Gaucher, C., Poulton, S. W., & Canfield, D. E. (2009). Fluctuations in Precambrian atmospheric oxygenation recorded by chromium isotopes. *Nature*, *461*(7261), 250–254. https://doi.org/10.1038/nature08266

Frei, R., Lehmann, B., Xu, L., & Frederiksen, J. A. (2020). Surface water oxygenation and bioproductivity—A link provided by combined chromium and cadmium isotopes in Early Cambrian metalliferous black shales (Nanhua Basin, South China). *Chemical Geology*, *552*, 119785. https://doi.org/10.1016/j.chemgeo.2020.119785

Horner, T. J., Little, S. H., Conway, T. M., Farmer, J. R., Hertzberg, J. E., Janssen, D. J., & GEOTRACES–PAGES Biological Productivity Working Group Members (2021). Bioactive trace metals and their isotopes as paleoproductivity proxies: An assessment using GEOTRACES-era data. *Global Biogeochemical Cycles*, *35*(11), e2020GB006814. https://doi.org/10.1029/2020GB006814

Huang, T., Moos, S. B., & Boyle, E. A. (2021). Trivalent chromium isotopes in the eastern tropical North Pacific oxygen-deficient zone. *Proceedings of the National Academy of Sciences of United States of America*, *118*(8), e1918605118. https://doi.org/10.1073/pnas.1918605118

Häusler, K., Dellwig, O., Schnetger, B., Feldens, P., Leipe, T., Moros, M., et al. (2018). Massive Mn carbonate formation in the Landsort Deep (Baltic Sea): Hydrographic prerequisites, temporal succession and Mn budget calculations. *Marine Geology*, *395*, 260–270. https://doi.org/10.1016/j.margeo.2017.10.010

Janssen, D. J., Rickli, J., Abbott, A. N., Ellwood, M. J., Twining, B. S., Ohnemus, D. C., et al. (2021). Release from biogenic particles, benthic fluxes, and deep water circulation control Cr and $\delta^{53}Cr$ distributions in the ocean interior. *Earth and Planetary Science Letters*, *574*, 117163. https://doi.org/10.1016/j.epsl.2021.117163

Janssen, D. J., Rickli, J., Quay, P. D., White, A. E., Nasemann, P., & Jaccard, S. L. (2020). Biological control of chromium redox and stable isotope composition in the surface ocean. *Global Biogeochemical Cycles*, *34*(1). https://doi.org/10.1029/2019GB006397

Lewis, B. L., & Landing, W. (1991). The biogeochemistry of manganese and iron in the Black Sea. *Deep-Sea Research A.*, *38*, S773–S803. https://doi.org/10.1016/S0198-0149(10)80009-3

Moos, S. B., Boyle, E. A., Altabet, M. A., & Bourbonnais, A. (2020). Investigating the cycling of chromium in the oxygen deficient waters of the Eastern Tropical North Pacific Ocean and the Santa Barbara Basin using stable isotopes. *Marine Chemistry*, *221*, 103756. https://doi.org/10.1016/j.marchem.2020.103756

Mugo, R. K. (1997). *The geochemistry of chromium in various marine environments*. PhD Thesis, University of British Columbia. https://doi.org/10.14288/1.0059582

Murray, J. W., Spell, B., & Paul, B. (1983). The contrasting geochemistry of manganese and chromium in the eastern tropical Pacific Ocean. In C. S. Wong, E. Boyle, K. W. Bruland, J. D. Burton, & E. D. Goldberg (Eds.), *Trace metals in sea water. NATO conference series (IV marine sciences)* (Vol. 9, pp. 643–669). Springer. https://doi.org/10.1007/978-1-4757-6864-0_37

Nasemann, P., Janssen, D. J., Rickli, J., Grasse, P., Franck, M., & Jaccard, S. L. (2020). Chromium reduction and associated stable isotope fractionation restricted to anoxic shelf waters in the Peruvian Oxygen Minimum Zone. *Geochimica et Cosmochimica Acta*, *285*, 207–224. https://doi.org/10.1016/j.gca.2020.06.027

Osborn, T. R., & Cox, C. S. (1972). Oceanic fine structure. *Geophysical Fluid Dynamics*, *3*(4), 321–345. https://doi.org/10.1080/03091927208236085

Planavsky, N. J., Reinhard, C. T., Wang, X., Thomson, D., McGoldrick, P., Rainbird, R. H., et al. (2014). Low Mid-Proterozoic atmospheric oxygen levels and the delayed rise of animals. *Science*, *346*(6209), 635–638. https://doi.org/10.1126/science.1258410

Rauret, G., López-Sánchez, J. F., Sahuquillo, A., Rubio, R., Davidson, C., Ure, A., & Quevauviller, P. (1999). Improvement of the BCR three step sequential extraction procedure prior to the certification of new sediment and soil reference materials. *Journal of Environmental Monitoring*, *1*(1), 57–61. https://doi.org/10.1039/A807854H

Reinhard, C. T., Planavsky, N. J., Robbins, L. J., Partin, C. A., Gill, B. C., Lalonde, S. V., et al. (2013). Proterozoic ocean redox and biogeochemical stasis. *Proceedings of the National Academy of Sciences of United States of America*, *110*(14), 5357–5362. https://doi.org/10.1073/pnas.1208622110

Reinhard, C. T., Planavsky, N. J., Wang, X., Fischer, W. W., Johnson, T. M., & Lyons, T. W. (2014). The isotopic composition of authigenic chromium in anoxic marine sediments: A case study from the Cariaco Basin. *Earth and Planetary Science Letters*, *407*, 9–18. https://doi.org/10.1016/j.epsl.2014.09.024

Richard, F. C., & Bourg, A. C. (1991). Aqueous geochemistry of chromium: A review. *Water Research*, *25*(7), 07–816. https://doi.org/10.1016/0043-1354(91)90160-R

Rickli, J., Janssen, D. J., Hassler, C., Ellwood, M. J., & Jaccard, S. L. (2019). Chromium biogeochemistry and stable isotope distribution in the southern ocean. *Geochimica et Cosmochimica Acta*, *262*, 188–206. https://doi.org/10.1016/j.gca.2019.07.033

Rudnick, R. L., & Gao, S. (2014). 4.1—Composition of the continental crust. In H. D. Holland & K. K. Turekian (Eds.), *Treatise on geochemistry* (2nd ed., pp. 1–51). Elsevier. https://doi.org/10.1016/B978-0-08-095975-7.00301-6

Rue, E. L., Smith, G. J., Cutter, G. A., & Bruland, K. W. (1997). The response of trace element redox couples to suboxic conditions in the water column. *Deep-Sea Research I.*, *44*(1), 113–134. https://doi.org/10.1016/S0967-0637(96)00088-X

Saggio, A., & Imberger, J. (2001). Mixing and turbulent fluxes in the metalimnion of a stratified lake. *Limnology & Oceanography*, *46*(2), 392–409. https://doi.org/10.4319/lo.2001.46.2.0392

Scheiderich, K., Amini, M., Holmden, C., & Francois, R. (2015). Global variability of chromium isotopes in seawater demonstrated by Pacific, Atlantic, and Arctic Ocean samples. *Earth and Planetary Science Letters*, *423*, 87–97. https://doi.org/10.1016/j.epsl.2015.04.030

Schoenberg, R., Zink, S., Staubwasser, M., & von Blanckenburg, F. (2008). The stable Cr isotope inventory of solid Earth reservoirs determined by double spike MC-ICP-MS. *Chemical Geology*, *249*(3–4), 294–306. https://doi.org/10.1016/j.chemgeo.2008.01.009

Sepúlveda Steiner, O., Bouffard, D., & Wüest, A. (2019). Convection-diffusion competition within mixed layers of stratified natural waters. *Geophysical Research Letters*, *46*(22), 13199–13208. https://doi.org/10.1029/2019GL085361

Sepúlveda Steiner, O., Bouffard, D., & Wüest, A. (2021). Persistence of bioconvection-induced mixed layers in a stratified lake. *Limnology & Oceanography*, *66*(4), 1531–1547. https://doi.org/10.1002/lno.11702

Sommer, T., Danza, F., Berg, J., Sengupta, A., Constantinescu, G., Tokyay, T., et al. (2017). Bacteria-induced mixing in natural waters. *Geophysical Research Letters*, *44*(18), 9424–9432. https://doi.org/10.1002/2017GL074868

Tonolla, M., Peduzzi, S., Hahn, D., & Peduzzi, R. (2003). Spatio-temporal distribution of phototrophic sulfur bacteria in the chemocline of meromictic Lake Cadagno (Switzerland). *FEMS Microbiology Ecology*, *43*(1), 89–98. https://doi.org/10.1111/j.1574-6941.2003.tb01048.x

Wang, X. (2021). The chromium isotope fractionation factor in seawater. *Chemical Geology*, *579*, 120358. https://doi.org/10.1016/j.chemgeo.2021.120358

Wanner, C., & Sonnenthal, E. L. (2013). Assessing the control on the effective kinetic Cr isotope fractionation factor: A reactive transport modeling approach. *Chemical Geology*, *337-338*, 88–98. https://doi.org/10.1016/j.chemgeo.2012.11.008

Wei, W., Klaebe, R., Ling, H. F., Huang, F., & Frei, R. (2020). Biogeochemical cycle of chromium isotopes at the modern Earth's surface and its applications as a paleo-environment proxy. *Chemical Geology*, *541*, 119570. https://doi.org/10.1016/j.chemgeo.2020.119570

Wüest, A. (1994). Interaktionen in seen: Die Biologie als Quelle dominanter physikalischer Kräfte. *Limnologica*, *24*(2), 93–104.

Xiong, Y., Guilbaud, R., Peacock, C. L., Cox, R. P., Canfield, D. E., Krom, M. D., & Poulton, S. W. (2019). Phosphorus cycling in Lake Cadagno, Switzerland: A low sulfate euxinic ocean analogue. *Geochimica et Cosmochimica Acta*, *251*, 116–135. https://doi.org/10.1016/j.gca.2019.02.011

References From the Supporting Information

Baker, M. A., & Gibson, C. H. (1987). Sampling turbulence in the stratified ocean: Statistical consequences of strong intermittency. *Journal of Physical Oceanography*, *17*(10), 1817–1836. https://doi.org/10.1175/1520-0485(1987)017<1817:STITSO>2.0.CO;2

Ball, J. W., & Bassett, R. L. (2000). Ion exchange separation of chromium from natural water matrix for stable isotope mass spectrometric analysis. *Chemical Geology*, *168*(1–2), 123–134. https://doi.org/10.1016/S0009-2541(00)00189-3

Cline, J. D. (1969). Spectrophotometric determination of hydrogen sulfide in natural waters. *Limnology & Oceanography*, *14*(3), 454–458. https://doi.org/10.4319/lo.1969.14.3.0454

Cole, D. B., Zhang, S., & Planavsky, N. J. (2017). A new estimate of detrital redox-sensitive metal concentrations and variability in fluxes to marine sediments. *Geochimica et Cosmochimica Acta*, *215*, 337–353. https://doi.org/10.1016/j.gca.2017.08.004

Crowe, S. A., O'Neill, A. H., Katsev, S., Hehanussa, P., Haffner, G. D., Sundby, B., et al. (2008). The biogeochemistry of tropical lakes: A case study from Lake Matano, Indonesia. *Limnology & Oceanography*, *53*(1), 319–331. https://doi.org/10.4319/lo.2008.53.1.0319

Davis, R. E. (1994). Diapycnal mixing in the ocean: The osborn–cox Model. *Journal of Physical Oceanography*, *24*(12), 2560–2576. https://doi.org/10.1175/1520-0485(1994)024<2560:DMITOT>2.0.CO;2

Dellwig, O., Wegwerth, A., Schnetger, B., Schulz, H., & Arz, H. W. (2019). Dissimilar behaviors of the geochemical twins W and Mo in hypoxic-euxinic marine basins. *Earth-Science Reviews*, *193*, 1–23. https://doi.org/10.1016/j.earscirev.2019.03.017

Farrell, Ú. C., Samawi, R., Anjanappa, S., Klykov, R., Adeboye, O. O., Agic, H., et al. (2021). The sedimentary geochemistry and paleoenvironments project. *Geobiology*, *19*(6), 545–556. https://doi.org/10.1111/gbi.12462

Goudsmit, G.-H., Peeters, F., Gloor, M., & Wüest, A. (1997). Boundary versus internal diapycnal mixing in stratified natural waters. *Journal of Geophysical Research*, *102*(C13), 27903–27914. https://doi.org/10.1029/97JC01861

Janssen, D. J., Rickli, J., Wille, M., Sepúlveda Steiner, O., Vogel, H., Dellwig, O., et al. (2022). Chemical data accompanying the manuscript "Chromium cycling in redox-stratified basins challenges δ^{53}Cr paleoredox proxy applications" in Geophysical Research Letters. (Version 1.0) [Dataset]. Zenodo. https://doi.org/10.5281/zenodo.7125831

Kwan, W. P., & Voelker, B. M. (2002). Decomposition of hydrogen peroxide and organic compounds in the presence of dissolved iron and ferrihydrite. *Environmental Science & Technology*, *36*(7), 1467–1476. https://doi.org/10.1021/es011109p

Luther, G. W., III, Church, T. M., & Powell, D. (1991). Sulfur speciation and sulfide oxidation in the water column of the Black Sea. *Deep-Sea Research*, *38*, S1121–S1137. https://doi.org/10.1016/S0198-0149(10)80027-5

Moos, S. B., & Boyle, E. A. (2019). Determination of accurate and precise chromium isotope ratios in seawater samples by MC-ICP-MS illustrated by analysis of SAFe Station in the North Pacific Ocean. *Chemical Geology*, *511*, 481–493. https://doi.org/10.1016/j.chemgeo.2018.07.027

Neaman, A., Mouélé, F., Trolard, F., & Bourrié, G. (2004). Improved methods for selective dissolution of Mn oxides: Applications for studying trace element associations. *Applied Geochemistry*, *19*(6), 973–979. https://doi.org/10.1016/j.apgeochem.2003.12.002

Sepúlveda Steiner, O., Carlino, C., Haizmann, E., Roman, S., Wüest, A., & Bouffard, D. (2022). Lake Cadagno 2017 CTD and water quality monitoring [Dataset]. Zenodo. https://doi.org/10.5281/zenodo.7127882

Shi, Z., Bonneville, S., Krom, M. D., Carslaw, K. S., Jickells, T. D., Baker, A. R., & Benning, L. G. (2011). Iron dissolution kinetics of mineral dust at low pH during simulated atmospheric processing. *Atmospheric Chemistry and Physics*, *11*(3), 995–1007. https://doi.org/10.5194/acp-11-995-2011

Sholkovitz, E. R., & Copland, D. (1982). The chemistry of suspended matter in Esthwaite Water, a biologically productive lake with seasonally anoxic hypolimnion. *Geochimica et Cosmochimica Acta*, *46*(3), 393–410. https://doi.org/10.1016/0016-7037(82)90231-9

Wei, W., Frei, R., Chen, T., Klaebe, R., Wei, G., Li, D., & Ling, H. (2018). Marine ferromanganese oxide: A potentially important sink of light chromium isotopes? *Chemical Geology*, *495*, 90–103. https://doi.org/10.1016/j.chemgeo.2018.08.006

Wirth, S. B., Gilli, A., Niemann, H., Dahl, T. W., Ravasi, D., Sax, N., et al. (2013). Combining sedimentological, trace metal (Mn, Mo) and molecular evidence for reconstructing past water-column redox conditions: The example of meromictic Lake Cadagno (Swiss Alps). *Geochimica et Cosmochimica Acta*, *120*, 220–238. https://doi.org/10.1016/j.gca.2013.06.017

Yamakawa, A., Yamashita, K., Makishima, A., & Nakamura, E. (2009). Chemical separation and mass spectrometry of Cr, Fe, Ni, Zn, and Cu in terrestrial and extraterrestrial materials using thermal ionization mass spectrometry. *Analytical Chemistry*, *81*(23), 9787–9794. https://doi.org/10.1021/ac901762a

Zhu, J. M., Wu, G., Wang, X., Han, G., & Zhang, L. (2018). An improved method of Cr purification for high precision measurement of Cr isotopes by double spike MC-ICP-MS. *Journal of Analytical Atomic Spectrometry*, *33*(5), 809–821. https://doi.org/10.1039/C8JA00033F